Cell

Genome-Scale CRISPR-Mediated Control of Gene Repression and Activation

Luke A. Gilbert,[1,2,3,4,8] Max A. Horlbeck,[1,2,3,4,8] Britt Adamson,[1,2,3,4] Jacqueline E. Villalta,[1,2,3,4] Yuwen Chen,[1,2,3,4] Evan H. Whitehead,[1,3,5,10] Carla Guimaraes,[6] Barbara Panning,[7] Hidde L. Ploegh,[6] Michael C. Bassik,[1,2,3,4,9] Lei S. Qi,[1,3,5,10] Martin Kampmann,[1,2,3,4,*] and Jonathan S. Weissman[1,2,3,4,*]
[1]Department of Cellular and Molecular Pharmacology
[2]Howard Hughes Medical Institute
University of California, San Francisco, San Francisco, CA 94158, USA
[3]California Institute for Quantitative Biomedical Research, San Francisco, CA 94158, USA
[4]Center for RNA Systems Biology, University of California, San Francisco, San Francisco, CA 94158, USA
[5]Center for Systems and Synthetic Biology, University of California, San Francisco, San Francisco, CA 94158, USA
[6]Department of Biology, Whitehead Institute for Biomedical Research and Massachusetts Institute of Technology, Cambridge, MA 02142, USA
[7]Department of Biochemistry and Biophysics University of California, San Francisco, San Francisco, CA 94158, USA
[8]Co-first author
[9]Present Address: Department of Genetics Stanford University, Palo Alto, CA, 94305, USA
[10]Present Address: Department of Bioengineering, Stanford University, Palo Alto, CA, 94305, USA
*Correspondence: martin.kampmann@ucsf.edu (M.K.), jonathan.weissman@ucsf.edu (J.S.W.)
http://dx.doi.org/10.1016/j.cell.2014.09.029

SUMMARY

While the catalog of mammalian transcripts and their expression levels in different cell types and disease states is rapidly expanding, our understanding of transcript function lags behind. We present a robust technology enabling systematic investigation of the cellular consequences of repressing or inducing individual transcripts. We identify rules for specific targeting of transcriptional repressors (CRISPRi), typically achieving 90%–99% knockdown with minimal off-target effects, and activators (CRISPRa) to endogenous genes via endonuclease-deficient Cas9. Together they enable modulation of gene expression over a ~1,000-fold range. Using these rules, we construct genome-scale CRISPRi and CRISPRa libraries, each of which we validate with two pooled screens. Growth-based screens identify essential genes, tumor suppressors, and regulators of differentiation. Screens for sensitivity to a cholera-diphtheria toxin provide broad insights into the mechanisms of pathogen entry, retrotranslocation and toxicity. Our results establish CRISPRi and CRISPRa as powerful tools that provide rich and complementary information for mapping complex pathways.

INTRODUCTION

Dramatic advances in sequencing technology have cataloged a universe of transcribed loci—greatly exceeding the number of canonical protein-coding open reading frames (ORFs)—which collectively are responsible for carrying out the instructions encoded by the genome (Djebali et al., 2012). A central challenge now is to understand the biological role of these transcripts and how quantitative differences in their expression define cellular states in normal development and in disease. Despite intense efforts, the function of many protein-coding genes remains poorly defined. Even less is known about the biological roles of most noncanonical transcripts such as enhancer RNAs, upstream antisense RNAs, lncRNAs, or other intergenic RNAs (Cech and Steitz, 2014). Efforts to address this deficiency in our knowledge would be greatly aided by techniques that are capable of dynamically and precisely controlling the expression of individual transcripts.

One way to explore the function of genes is to disrupt their expression through repression. The dominant tool for programmed knockdown of mRNAs is RNA interference (RNAi) (Chang et al., 2006). However, RNAi has pervasive problems with off-target effects, which can be especially confounding in the context of large-scale screens (Adamson et al., 2012; Jackson et al., 2003; Sigoillot et al., 2012). Additionally, because RNAi is mediated by cytoplasmic argounaute proteins, gene silencing through this approach is best suited to depletion of cytosolic mRNA targets.

An alternative emerging strategy is the use of programmable genome editing methods that permanently delete or modify DNA using designable, sequence-specific endonucleases such as zinc finger, transcription activator-like effector (TALE) nucleases, or CRISPR (*c*lustered *r*egularly *i*nterspaced *s*hort *p*alindromic *r*epeats)/Cas9 (CRISPR-associated protein 9) proteins (Gaj et al., 2013; Sander and Joung, 2014). A series of elegant studies recently exploited the readily programmable nature of Cas9, in which the specificity is determined by a short guide (sg)RNA, to enable genome-scale loss-of-function screens (Koike-Yusa et al., 2014; Shalem et al., 2014; Wang et al., 2014). These studies established CRISPR-mediated cutting as a powerful screening technology complementary to RNAi and haploid mutagenesis screens (Carette et al., 2009). Nonetheless, screening approaches

based on genome editing are currently focused on loss-of-function studies involving irreversible frameshift disruptions, limiting their utility for the study of essential genes and long noncoding RNAs. Additionally, double-stranded DNA breaks can be cytotoxic (Huang et al., 1996; Jackson, 2002). Finally, indels formed from error-prone DNA repair are often short and in-frame, which could limit the ability to disable all of the alleles of a gene.

A programmable DNA-binding protein that can recruit an effector domain to turn transcription on and off in a dynamic and quantitative manner offers, in principle, a more flexible tool for interrogating the many transcripts in complex genomes. Pioneering experiments with designed chimeric zinc finger and TALE proteins fused to transcription effector domains demonstrate that such an approach can modulate transcription of endogenous genes (Beerli et al., 1998, 2000; Zhang et al., 2011). However, as each transcript target requires a unique fusion protein, expanding these methods to genome-scale is arduous.

Recently, we and others have used catalytically inactive Cas9 (dCas9) fusion proteins guided by gene-specific sgRNAs to localize effector domains to specific DNA sequences to either repress (CRISPRi) or activate (CRISPRa) transcription of target genes (Gilbert et al., 2013; Sander and Joung, 2014). To date, a small number of sgRNAs have been tested, leaving unanswered whether CRISPRi/a is a feasible strategy for globally interrogating gene function and, if so, how best to target a gene to activate or repress transcription while minimizing off-target effects.

Here, we describe the development and application of a method for high-specificity, genome-scale modulation of transcription of endogenous genes in human cells using CRISPRi/a. To accomplish this, we first performed a saturating screen in which we tested the activity of every unique sgRNA broadly tiling around the transcription start sites (TSSs) of 49 genes known to modulate cellular susceptibility to ricin (Bassik et al., 2013). From this, we extracted distinct rules for regions where either CRISPRi or CRISPRa maximally changes the expression of endogenous genes, as well as rules for predicting off-target effects, providing an algorithm to design two genome-scale libraries targeting each gene with 10 sgRNAs. We validated these libraries by screening for genes that control cell growth and response to a chimeric cholera/diphtheria fusion toxin (CTx-DTA) (Guimaraes et al., 2011). These experiments demonstrate that our CRISPRi/a screening platform is robust, showing high reproducibility and activity with undetectable intrinsic toxicity. More generally, we establish that transcriptional repression is inducible, reversible, and can target essential genes. We demonstrate that we can use CRISPRi and CRISPRa to control transcript levels for endogenous genes across a wide dynamic range. We also provide extensive evidence that properly designed CRISPRi reagents are highly specific. As such, these methods represent transformative tools for defining transcript function across the breadth of transcripts encoded by the human genome.

RESULTS

A High-Throughput Tiling Screen Defines Rules for CRISPRi Activity at Endogenous Genes

CRISPRi can repress transcription by directly blocking RNA polymerase activity (dCas9) or through effector domain-mediated transcriptional silencing (dCas9-KRAB) (Gilbert et al., 2013; Qi et al., 2013). In order to better understand and optimize CRISPRi activity, we used a pooled high-throughput screen to define rules that determine CRISPRi repression of endogenous genes. We targeted 49 genes that we had previously shown to modulate cellular susceptibility to the AB toxin ricin (Bassik et al., 2013). The extent of gene repression for these genes typically has a monotonic relationship with the ricin-resistance phenotype, allowing us to use a ricin-resistance score calculated by monitoring sgRNA frequencies in a pooled screen to indirectly measure transcriptional repression.

Using massively parallel oligonucleotide synthesis, we generated a library of sgRNAs that tile the DNA in a 10-kilobase window around the TSS of these 49 genes (54,810 total sgRNAs) (Bassik et al., 2009) (Figure 1A). We also included 1,000 negative control sgRNAs derived from scrambled sequences corresponding to the same windows.

We packaged this tiling library of sgRNAs into lentiviral particles and transduced K562 human myeloid leukemia cells stably expressing dCas9 or a dCas9-KRAB fusion protein, which we have previously described (Gilbert et al., 2013). We harvested populations of cells expressing the library either at the outset of the experiment, after growth under standard conditions, or following ricin treatment. We then counted the frequency of each sgRNA in the library in each sample using deep sequencing to determine how each sgRNA in the library modulates cell growth and cellular susceptibility to ricin phenotypes. We defined these phenotypes quantitatively as gamma (γ) and rho (ρ), respectively (See Figure S1A, available online, and Kampmann et al., 2013).

Many sgRNAs potently repress gene expression, as evidenced by their impact on ricin sensitivity (Figures 1B and S2A). Plotting this data for all 49 genes showed that active sgRNAs cluster around or just downstream from the TSS of each gene for dCas9-KRAB and dCas9, respectively (Figure 1C). We saw that strong CRISPRi activity is obtained by targeting dCas9-KRAB to a window of DNA from -50 to +300 bp relative to the TSS of a gene, with a maximum in the $\sim$50–100 bp region just downstream of the TSS (Figures 1C and 1D). This suggested that optimal activity leverages the combined activity of dCas9 interference along with repression from the KRAB domain. We also observed that sgRNAs with protospacer lengths of 18–21 base pairs were significantly more active than sgRNAs containing longer protospacers (Figure S2B). Nucleotide homopolymers had a strongly negative effect on sgRNA activity (Figure S2D). However, neither the DNA strand that was targeted nor the sgRNA GC content across a broad range strongly correlated with sgRNA activity (Figures S2C and S2E).

To evaluate the feasibility of genome-scale genetic screens based on CRISPRi, we compared the strength of phenotypes obtained with CRISPRi to our previously published shRNA data. We applied the rules described above to data from our sgRNA tiling library to select all sgRNAs predicted to be highly active and then randomly subsampled sets of 10 or 24 sgRNAs. We calculated a normalized phenotype Z score by dividing mean phenotypes for each gene by the standard deviation of sgRNA phenotypes from the nontargeting control set (Figure S1B). We see significant ricin phenotypes for each of the 49 genes. Moreover, in virtually every case the normalized ricin phenotype

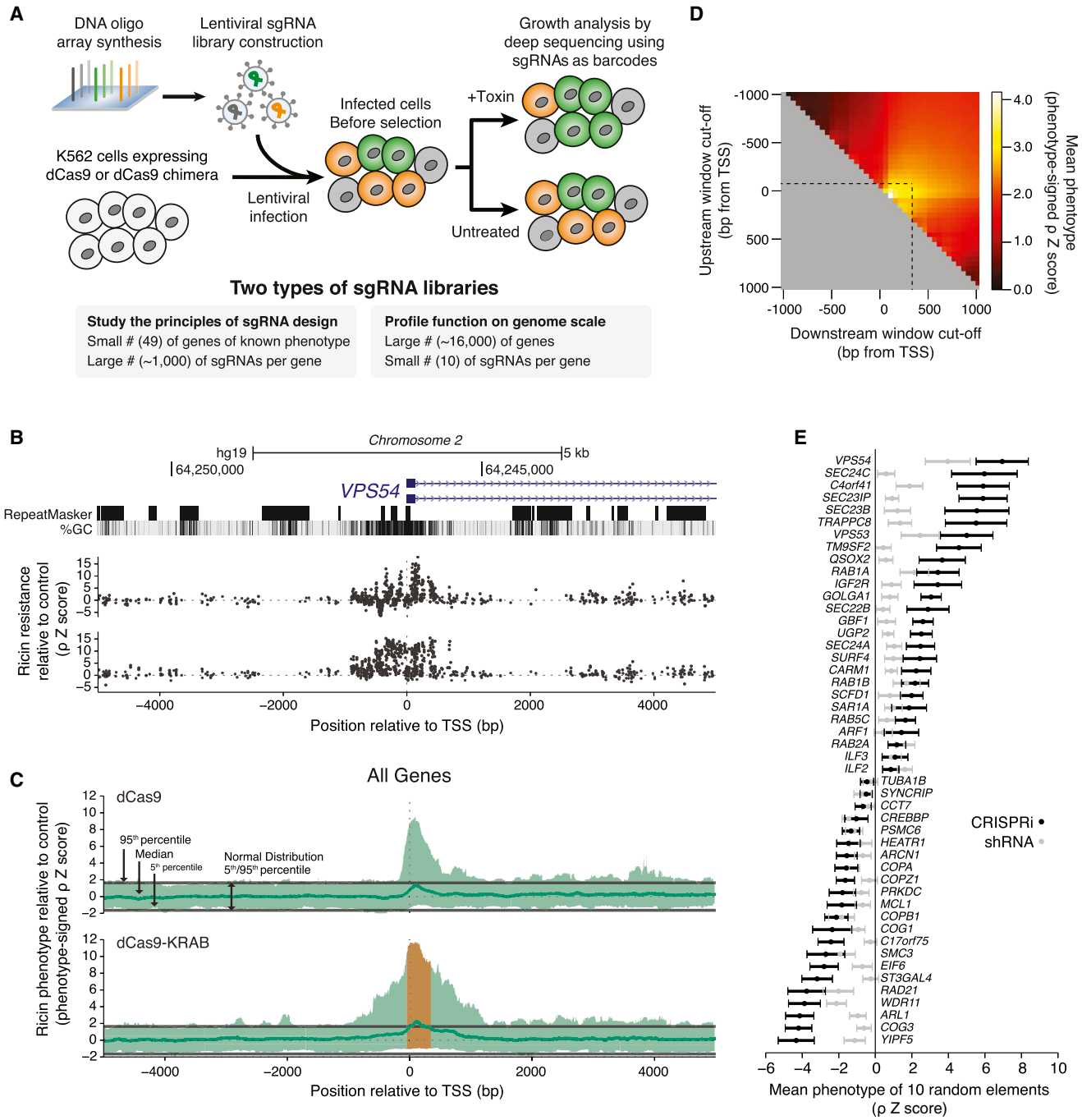

Figure 1. A Tiling sgRNA Screen Defines Rules for CRISPRi Activity at Endogenous Genes in Human Cells

(A) Massively parallel determination of growth or toxin-resistance phenotypes caused by sgRNAs in mammalian cells expressing dCas9 or dCas9 fusion constructs.

(B) UCSC genome browser tracks showing the genomic organization, GC content, and repetitive elements around the TSS of a representative gene, *VPS54*, across a 10 kb window targeted by the tiling sgRNA library. sgRNA ricin-resistance phenotypes (as Z scores, see Figure S1 and Experimental Procedures) in dCas9 and dCas9-KRAB expressing K562 cells are depicted in black on the top and bottom, respectively. See also Figure S2A for more examples.

(C) Sliding-window analysis of all 49 genes targeted in a tiling sgRNA library. Green line: median sgRNA activity in a defined window for all genes. Orange region: observed average window of maximum CRISPRi activity. Data displayed as a phenotype signed Z score, excluding all guides longer than 22 bp.

(D) CRISPRi activity for all 49 genes in defined windows relative to the TSS of each gene.

(E) Ricin-resistance phenotypes, comparing CRISPRi sgRNAs selected by our rules to RNAi, for genes previously established to cause ricin-resistance phenotypes when knocked down by RNAi. Mean ± SD phenotype-signed Z score of 100 sets of 10 randomly subsampled sgRNAs or shRNAs. See also Figure S2F.

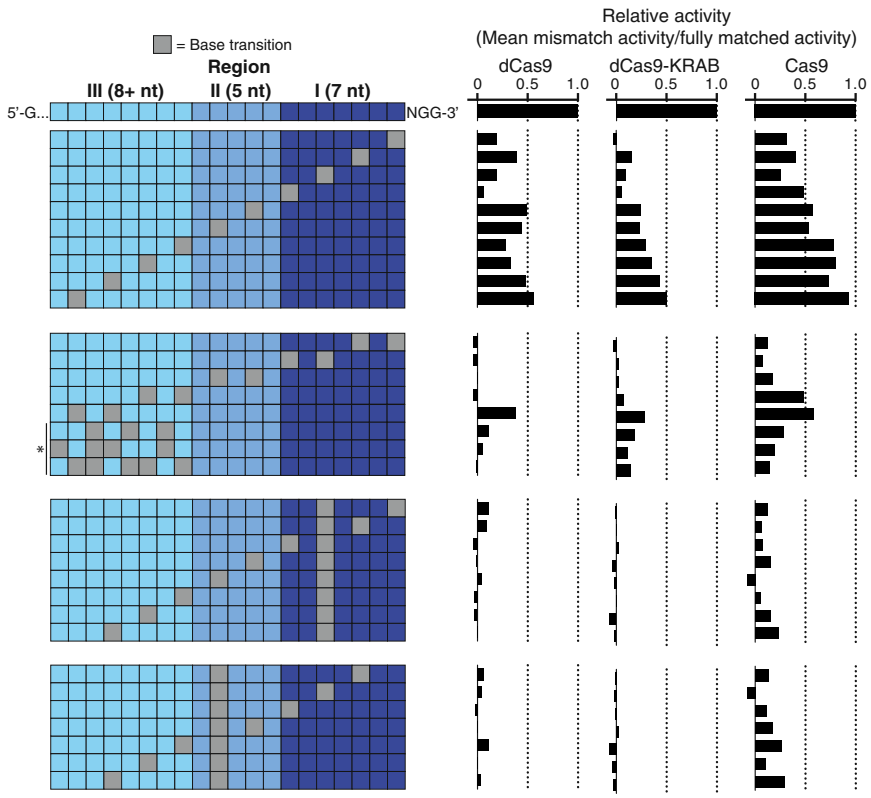

Figure 2. CRISPRi Activity is Highly Sensitive to Mismatches Between the sgRNA and DNA sequence

On- and off-target activity of dCas9, dCas9-KRAB and Cas9 for sgRNAs with a varying number and position of mismatches. Off-target activity of sgRNAs with mismatches is displayed as percent of the on-target activity for the corresponding sgRNA without mismatches. Asterisk indicates sgRNAs with three, four, or five mismatches randomly distributed across region 3 of the sgRNA sequence. Data are displayed for each mismatch position as the mean of all sgRNAs with that mismatch; see Figure S3 for individual sgRNA activities. sgRNAs were included in the analysis only if the fully matched guide was highly active (phenotype-signed Z score $\geq$ 4); n = 5 for dCas9, n = 11 for dCas9-KRAB, and n = 10 for Cas9.

Z score or p value is stronger (in many cases far stronger) than seen with a comparably-sized shRNA library (generated by subsampling our published data) (Figures 1E and S2F).

CRISPRi Transcriptional Silencing Is Highly Sensitive to Mismatches between the Target DNA Site and the sgRNA

To assess CRISPRi off-target activity at endogenous genes, we selected a set of 30 sgRNAs from our tiling library (6 sgRNAs/gene targeting five genes). For each of these sgRNAs, we tested the activity of a series of derivative sgRNAs with a variable number and position of mismatches (Figure 2). This experiment allowed us to measure the relative amount of gene repression for sgRNAs with or without mismatch base pairing targeting the same DNA locus. We found that even a single mismatch at the 3′ end of the protospacer decreased CRISPRi activity on average, while combinations of mismatches that pass our off-target filter abolished activity (Figures 2, and S3, and Extended Experimental Procedures). From this analysis, we concluded that properly designed CRISPRi sgRNAs have minimal off-target transcriptional repression activity.

A High-Throughput Tiling Screen Defines Rules for CRISPRa Activity at Endogenous Genes

We recently developed an improved CRISPRa method, termed sunCas9, in which expression of a single sgRNA with one binding site is sufficient to robustly activate transcription (Tanenbaum et al., 2014, this issue). In the sunCas9 system, a single dCas9 fusion protein bound to DNA recruits multiple copies of the activating effector domain, thus amplifying our ability to induce transcription (Figure 3A).

To define rules for optimal CRISPRa sgRNA design, we used our tiling library, which targets genes capable of modulating cellular sensitivity to ricin. We previously showed for several of the genes in this tiling library that knockdown and plasmid overexpression resulted in opposite ricin phenotypes (Bassik et al., 2013). For example, knockdown of *SEC23B* sensitized cells to ricin, whereas *SEC23B* overexpression desensitized cells to ricin. These observations suggested that we should be able to observe reversed phenotypes in this tiling screen arising from CRISPRa activity.

We transduced K562 cells stably expressing the sunCas9 system (Figure 3A) with the sgRNA tiling library and screened for ricin phenotypes as described for CRISPRi above. Analysis of data for individual genes or averaged data for all 49 genes demonstrated that many sgRNAs for each gene affected ricin resistance (Figures 3B, S4A, and S4B). Our negative control sgRNAs showed very little activity and were not correlated between biological replicate screens, suggesting that CRISPRa activity is specific. We observed a peak of active sgRNAs for CRISPRa at −400 to −50 bp upstream from the TSS (Figure 3B). This activity pattern fits with a model in which each VP16 domain can bind the mediator complex and recruit basal transcription machinery, activating transcription when spaced appropriately from a TSS (Mittler et al., 2003). With this system, we have shown we can turn on genes that are poorly expressed and increase the expression of well-expressed genes (Figure 3E). Overall, our CRISPRi/a tiling screens provide rules for how CRISPRi/a controls expression of endogenous genes.

An Allelic CRISPRi/a Series of Transcript Activation and Repression Shows that Protein Abundance Dynamically Modulates the Cellular Response to Ricin

For many genes, we do not know how the relative abundance of the encoded protein relates to its function. We observed a

marked anticorrelation in our ricin screens between CRISPRa phenotypes and CRISPRi phenotypes for individual genes (Figure 3C). As the genes targeted by our tiling library were selected based on a knockdown phenotype, all genes showed phenotypes in the CRISPRi screen, but only a subset showed phenotypes in the CRISPRa screen.

To validate results from both the CRISPRi and CRISPRa tiling screens, we selected an allelic series of sgRNAs by phenotype from the screen and retested each sgRNA individually (38 sgRNAs targeting four genes). Our results show that our CRISPRi/a screens produced reliable phenotype scores, robustly reproduced upon retesting, and that CRISPRi/a can activate and repress the transcription of endogenous genes over a wide dynamic range (up to ~1,000-fold) (Figures 3D and 3E), enabling systematic interrogation of how gene dosage controls cellular functions of interest.

A Robust and Highly Specific Genome-Scale CRISPRi Screening Platform

The results of our tiling CRISPRi screen established our ability to pick active sgRNAs with low off-target activity and provided a set of rules enabling us to design a robust genome-scale sgRNA library. We chose a library size of 10 sgRNAs/gene for the following reasons. Over half of the sgRNAs conforming to these rules gave clear ricin phenotypes. For a library with 10 sgRNAs/gene, 94% of the genes would thus have 2 or more highly active sgRNAs. Finally, computational subsampling of the phenotypic data from our tiling library data to 10 sgRNAs/gene and calculation of Z scores for hit genes indicated that a library with 10 sgRNAs/gene would reliably detect hit genes (Figure 1E).

We synthesized and cloned a genome-scale CRISPRi sgRNA library targeting 15,977 human protein-coding genes (10 sgRNAs/TSS, targeting 20,898 TSS) with 11,219 nontargeting control sgRNAs for a total of 206,421 sgRNAs (Table S2). To evaluate this library, we first screened for genes essential for cell growth in K562 cells. Briefly, K562 cells stably expressing dCas9-KRAB were transduced in replicate with the entire genome-scale library, and each replicate was grown for 10 days at a minimum library coverage of 3,750 cells/sgRNA in a single spinner flask.

To characterize our screening methodology and library design, we examined the correlation between screen replicates. Individual sgRNAs reproducibly showed dramatic depletion (up to 256-fold) over a 10 day screen, demonstrating that individual sgRNAs can have profound effects on cell growth (Table S2) (Figure 4A). The distribution of our negative control sgRNAs was very narrow with little correlation between replicates (Spearman R = 0.036), suggesting that the off-target activity of these controls is very low (Figure 4A). Indeed, 99.7% of our negative controls had no detectable activity. The observed specificity is consistent with our previously published RNA-seq data (Gilbert et al., 2013).

To further explore the prevalence of off-target effects, we examined two classes of genes not expected to show any on-target activity in our screen: olfactory receptors and genes on the Y chromosome. The sgRNAs that target these genes were designed and picked in the same manner as the rest of the library; however, olfactory receptors should not be expressed in this cell type and, as K562 cells are derived from a female donor, sgRNAs that target genes on the Y chromosome lack a DNA target. As with the negative controls, these genes show no phenotype on average and exhibit very little correlation between replicates (Spearman R = 0.057 for olfactory genes and −0.052 for Y targeting) (Figure 4A). We also observed no evidence of nonspecific toxicity due to expression of dCas9-KRAB and our sgRNA library in K562 cells, suggesting that dCas9 bound to the genome is not toxic under these conditions (Figure 4B). Thus, CRISPRi is highly specific and nontoxic.

To identify hit genes in this screen, we used a metric of average growth phenotype (γ) for the top three sgRNAs for each gene (see Experimental Procedures and Table S3). Among the top hits were genes involved in essential cellular functions, including translation, transcription, and DNA replication (Figures 4C and S5A) (Huang et al., 2009a, 2009b), thus validating our approach as a screening platform.

A Genome-Scale CRISPRa Screening Platform

The results of our CRISPRa tiling screen established our ability to confidently measure gene phenotypes resulting from inducing expression with single sgRNAs. As with the CRISPRi tiling screens, our data enabled the development of a set of rules that allowed construction of a genome-scale CRISPRa library. Many of these rules overlapped with those of CRISPRi (e.g., sgRNA length and sequence preferences). A key difference is that the optimal window for targeting sgRNAs for CRISPRa lies upstream of the TSS (Figure 3B). We therefore constructed an independent CRISPRa library, designing 10 sgRNAs between −400 to −50 base pairs upstream of each TSS for 15,977 human genes, along with 5,968 nontargeting control sgRNAs, for a total of 198,810 sgRNAs.

We evaluated our CRISPRa platform in a screen for genes that affect cell growth when induced in K562 cells constitutively expressing the sunCas9 system. Replicate screens were conducted as described above. The magnitude of growth defects seen in our CRISPRa screen was comparable to that of the above CRISPRi screen, although fewer sgRNAs caused a growth phenotype (Figure S5B and Table S2). We analyzed control sgRNAs with no genomic target or Y chromosome targets and found minimal phenotypes, which lacked substantial correlation between experimental replicates (Spearman R = 0.155 and R = 0.010, respectively), indicating that the phenotype distribution observed in nontargeting controls was primarily a result of stochastic noise rather than off-target effects. Furthermore, the fraction of cells expressing sgRNAs and the sunCas9 system was stable over the course of the experiment, indicating that there was no general toxicity associated with the CRISPRa platform (Figure 4B). These data suggest that, like CRISPRi, CRISPRa is specific and nontoxic.

Defining Regulators of Survival and Differentiation in Human Cells by CRISPRa

We then investigated the genes whose induction caused cells to deplete over the course of our CRISPRa screen. We scored genes by the average γ of the three most active sgRNAs as above, and compared these phenotypes to those observed in the CRISPRi screen (Figure 4D and Table S3). The results from the two screens had little overlap, suggesting that few genes

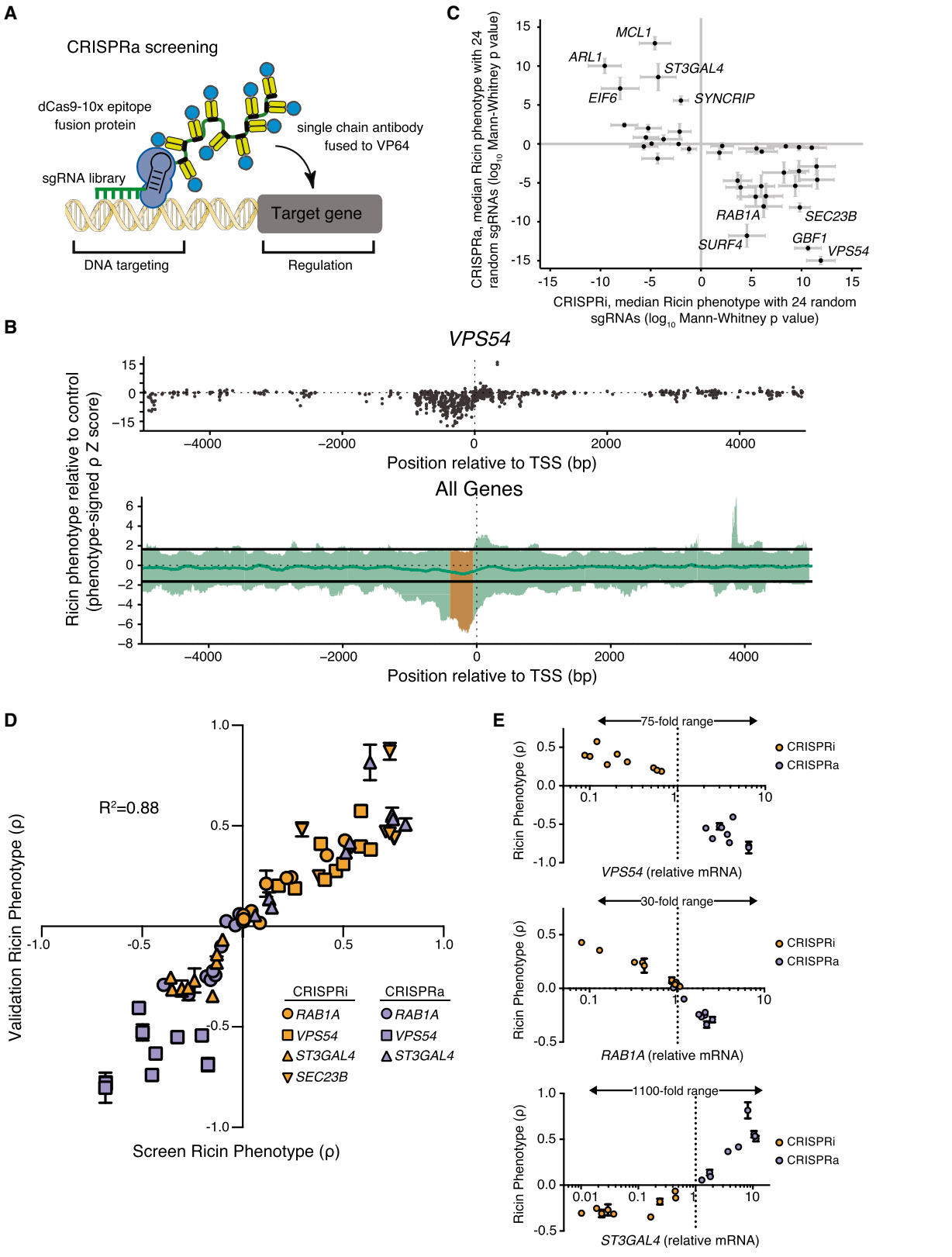

(legend on next page)

are both essential and toxic upon induction and that wild-type expression levels of genes are generally optimal for K562 growth. Whereas CRISPRi hits are naturally limited to expressed genes, CRISPRa hits included genes across a broad range of endogenous expression levels (Figure S5D). We observed that the majority of genes that inhibited growth in the CRISPRa screen fell into three overlapping classes.

The first class was tumor suppressor genes: 18 of the top 50 genes, including six of the top seven, are known to have potent tumor suppressor activity (Vogelstein et al., 2013; Zhao et al., 2013). These genes include p53-related protein *TP73*, cell cycle inhibitors *CDKN1C* (p57) and *CDKN1A* (p21), apoptotic factors *BAK1* and *BCL2L11* (BIM), and chromatin remodeling factor *ARID1A* (Figure 4D and Table S4). Gene set enrichment analysis (GSEA) confirmed this observation, highlighting several genes important in the intrinsic pathway of apoptosis or in chronic myeloid leukemia (CML) homeostasis consistent with the origin of K562 cells as a clonal isolate from a CML blast crisis (ATCC) (Figure 4E). Similarly, top gene ontology annotations included "positive regulation of apoptosis" and "regulation of cell cycle" (Figure S5C). While tumor suppressors are classically considered to be mutated early in cancer progression (Vogelstein et al., 2013), these results demonstrate than many potential tumor suppressor genes remain functional but downregulated and suggest that CRISPRa can be used to pinpoint intact pathways and vulnerabilities in tumor cells.

Transcription factor families with well-established roles in tissue development and differentiation represent another class of growth hits, accounting for 16 of the top 50 genes (K562 cells have known potential to undergo erythroid differentiation). These genes include CCAAT/Enhancer-binding proteins (CEBP), Homeobox genes, Forkhead box genes, Ikaros family zinc finger proteins, and hematopoietic differentiation factor *SPI1* (PU.1) (Figure 4D and Table S4) (Spitz and Furlong, 2012). This observation is reflected in enriched annotations relating to multicellularity, cell differentiation, and development (Figure S5C).

The complementary nature of the CRISPRi and CRISPRa screens is nicely illustrated by results from two gene pairs (*SPI1*/*GATA1* and *CEBPA*/*CEBPG*) in which one member of each pair inhibits the function of the other. *GATA1* and *CEBPG* were strong hits in the CRISPRi screen, consistent with their roles as inhibitors of myeloid differentiation. By contrast, both *SPI1* and *CEBPA* were robust hits in our CRISPRa activation screen. These observations are consistent with the inhibitory functions of *SPI1* and *CEBPA*: silencing of *CEBPA* leads to derepression of *CEBPG* (Alberich-Jordà et al., 2012) and the protein encoded by *SPI1* (PU.1) is a direct binding partner of GATA-1 and inhibits its transcriptional activity (Zhang et al., 2000).

Finally, several hit genes have key roles in mitosis. *PLK4* controls centrosome duplication, and overexpression of the gene in U2OS cells leads to increased centriole number (Habedanck et al., 2005). The proteins encoded by *KIF18B* and *KIF2C* form a complex that destabilizes microtubules during mitosis (Tanenbaum et al., 2011).

Overall, the results from our paired CRISPRi/a growth screens demonstrate that complementary information can be obtained by loss- and gain-of-function genetic screens, and highlight the utility of the platform for future studies into tumor biology and cell differentiation.

Dynamically Controlling Gene Expression with CRISPRi

The ability to reversibly tune the expression of select transcripts would be a powerful tool for evaluating transcript function. To evaluate the applicability of CRISPRi to this purpose, we cloned a lentiviral expression construct that places an optimized KRAB-dCas9 fusion protein under the control of a doxycycline-inducible promoter (Figures 5A and 5B). Induced expression of KRAB-dCas9 robustly depletes transcript levels from sgRNA-targeted genes (Figures 5C and S5E). To further assess dynamic control of CRISPRi, we inducibly repressed several genes identified in our genome-scale CRISPRi growth screen (Figure S5G). Cells that express sgRNAs targeting these essential genes showed almost no growth phenotype in the absence of doxycycline, but rapidly and robustly disappeared from the population upon addition of doxycycline (Figure 5D). Additionally, gene repression and resulting phenotypes were reversible (Figures 5C, S5E, and S5F), indicating that KRAB-dCas9 does not create a permanently repressive chromatin state at targeted promoters.

To test our ability to dynamically control expression of essential genes on a larger scale, we cloned a sublibrary targeting 426 manually curated genes (10 sgRNAs/TSS or 4,923 targeting sgRNAs plus 750 nontargeting controls). This library was transduced into K562 cells stably expressing our inducible KRAB-dCas9 fusion protein, and cell growth effects were then evaluated in the presence and absence of doxycycline. Only four sgRNAs were depleted strongly in the absence of doxycycline; however, with induction of KRAB-dCas9, many sgRNAs were strongly depleted (Figure 5E). Negative control sgRNAs again

Figure 3. A Tiling sgRNA Screen Defines Rules for CRISPRa Activity at Endogenous Genes in Human Cells

(A) A schematic of the dCas9-SunTag + scFV-VP64 + sgRNA system for CRISPRa.

(B) Activity of sgRNAs in K562 cells stably expressing each component of CRISPRa, as a function of the distance of the sgRNA site to the TSS of the targeted gene (Phenotype-signed Z scores; therefore, negative values represent opposite results than from knockdown). Top, sgRNAs targeting *VPS54*; Bottom, sliding-window analysis of all 49 genes targeted by our tiling library in green. Green line, median activity; orange, window of maximal activity. Guides longer than 22 bp were excluded. See also Figure S4.

(C) CRISPRa phenotypes and CRISPRi (dCas9-KRAB) phenotypes are anticorrelated for select genes. For each gene, a Mann-Whitney p value is calculated using CRISPRi/a sgRNA activity relative to a negative control distribution for 24 subsampled sgRNAs. Mean ± SD p value of 100 randomly subsampled sets is displayed.

(D) CRISPRi knockdown and CRISPRa activation of the same gene can have opposing effects on ricin resistance in both primary screens and single sgRNA validation experiments (mean ± SD of 3 replicates).

(E) Modulation of expression levels for 3 genes by CRISPRi and CRISPRa as quantified by qPCR plotted against the ricin-resistance phenotype (mean ± SD of 3 replicates) measured for each sgRNA.

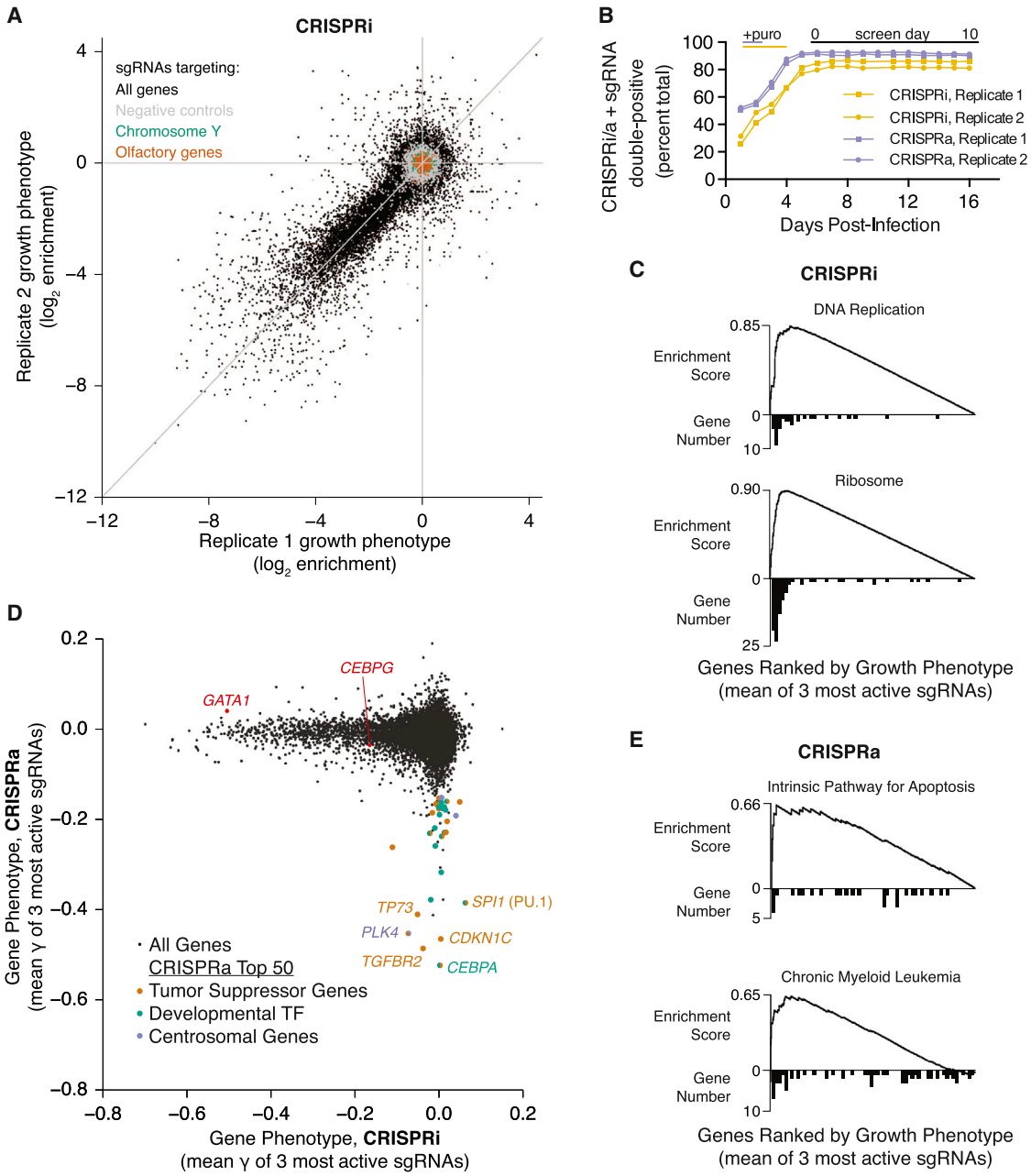

Figure 4. Genome-Scale CRISPRi and CRISPRa Screens Reveal Genes Controlling Cell Growth

(A) sgRNA phenotypes from a genome-scale CRISPRi screen for growth in human K562 cells (black). Three classes of negative control sgRNAs are color-coded: nontargeting sgRNAs (gray), sgRNAs targeting Y-chromosomal genes (green) and sgRNAs targeting olfactory genes (orange).

(B) Coexpression of sgRNAs and dCas9-KRAB or dCas9-SunTag + scFV-VP64 is not toxic in K562 cell lines over 16 days.

(C) Gene set enrichment analysis (GSEA) for hits from the CRISPRi screen. A histogram of gene distribution is shown under the GSEA curve.

(D) CRISPRi versus CRISPRa gene phenotypes for genome-scale growth screens (black). For the 50 genes in the CRISPRa screen with the most negative growth phenotype, each gene was annotated and labeled based on evidence of activity as a tumor suppressor (orange), developmental transcription factor (green), or in regulation of the centrosome (purple). Two additional CRISPRi hit genes that are discussed in the text are labeled in red. See Table S4 for annotations and references.

(E) GSEA for hits from the CRISPRa growth screen. A histogram of gene distribution is shown under the GSEA curve.

produced a narrow distribution of phenotypes with little correlation between biological replicates with or without doxycycline. Additionally, we found no evidence that targeted KRAB-dCas9 generally impedes cell growth (Figure 5F). Taken together, these results demonstrate CRISPRi is nontoxic, inducible and reversible.

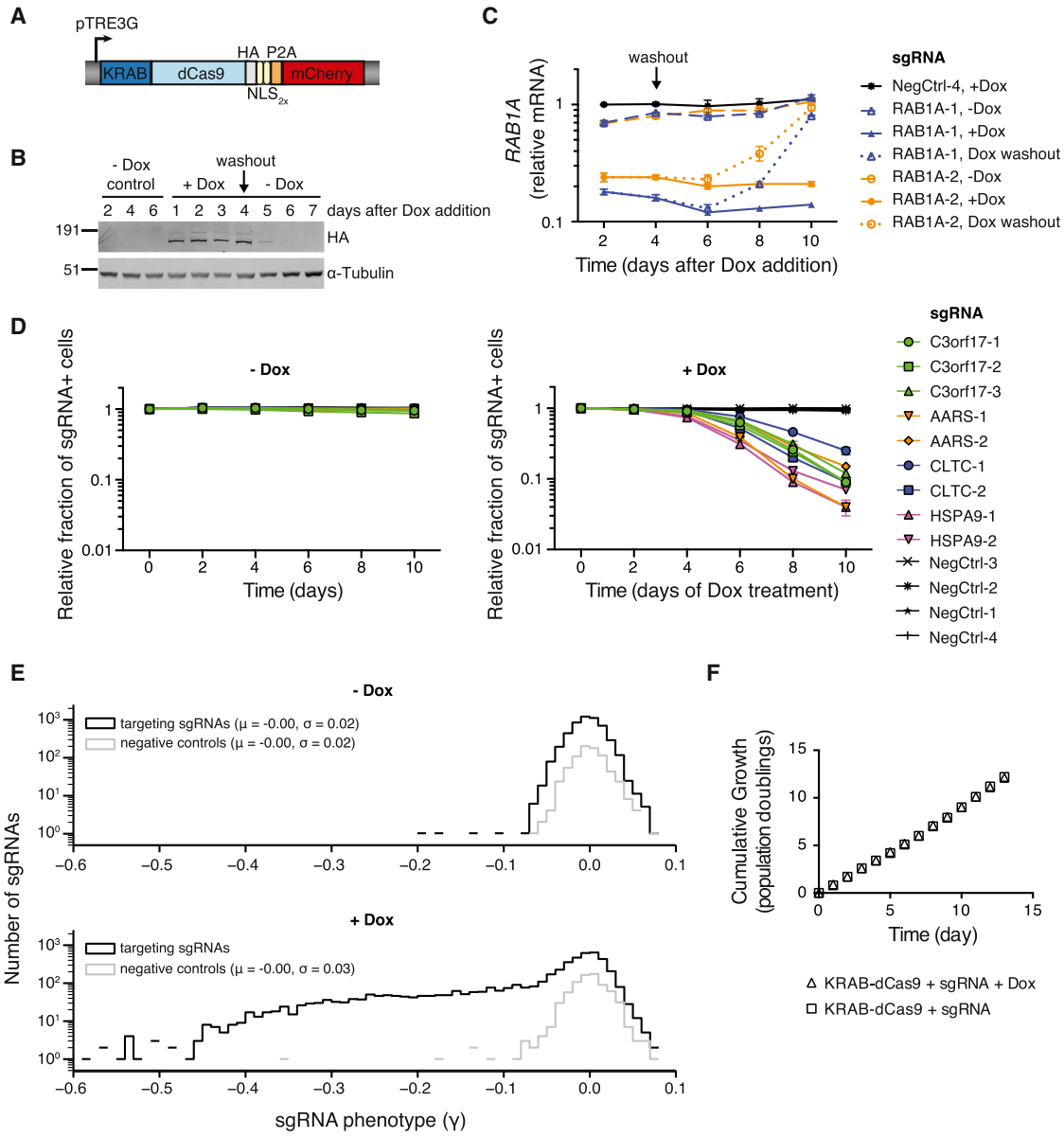

Figure 5. CRISPRi Gene Silencing Is Inducible, Reversible, and Nontoxic

(A) Expression construct encoding an inducible KRAB-dCas9 fusion protein.

(B) Western blot analysis of inducible KRAB-dCas9 in the absence, presence, and after washout of doxycycline.

(C) Relative *RAB1A* expression levels (as quantified by qPCR) in inducible CRISPRi K562 cells transduced with *RAB1A*-targeting sgRNAs in the absence, presence, and after washout of doxycycline. Mean ± standard error of technical replicates (n = 2) normalized to control cells (assayed in the presence of doxycycline) from the day 2 time point.

(D) Competitive growth assays performed with inducible CRISPRi K562 cells transduced with the indicated sgRNAs in the presence and absence of doxycycline. Data are represented as the mean ± SD of replicates (n = 3). See also Figure S5G.

(E) A CRISPRi sublibrary screen for effects on cell growth was performed with inducible CRISPRi K562 cells in the presence and absence of doxycycline.

(F) Cumulative growth curves from the sublibrary screen represented in (E) show no bulk changes to growth caused by induction of KRAB-dCas9. Mean ± SD of replicate infections each screened in duplicate.

A Genome-Scale CRISPRi Screen Reveals Pathways and Complexes that Govern Response to Cholera and Diphtheria Toxin

To test the performance of our CRISPRi approach for detecting genes controlling a more complex cellular phenotype, we performed a genome-scale CRISPRi screen for genes that modulate sensitivity to a chimeric toxin composed of the diphtheria toxin catalytic A subunit covalently linked to cholera toxin (CTx-DTA, Figure 6A). This chimera had been previously developed to provide a growth readout for cholera intoxication (Guimaraes et al.,

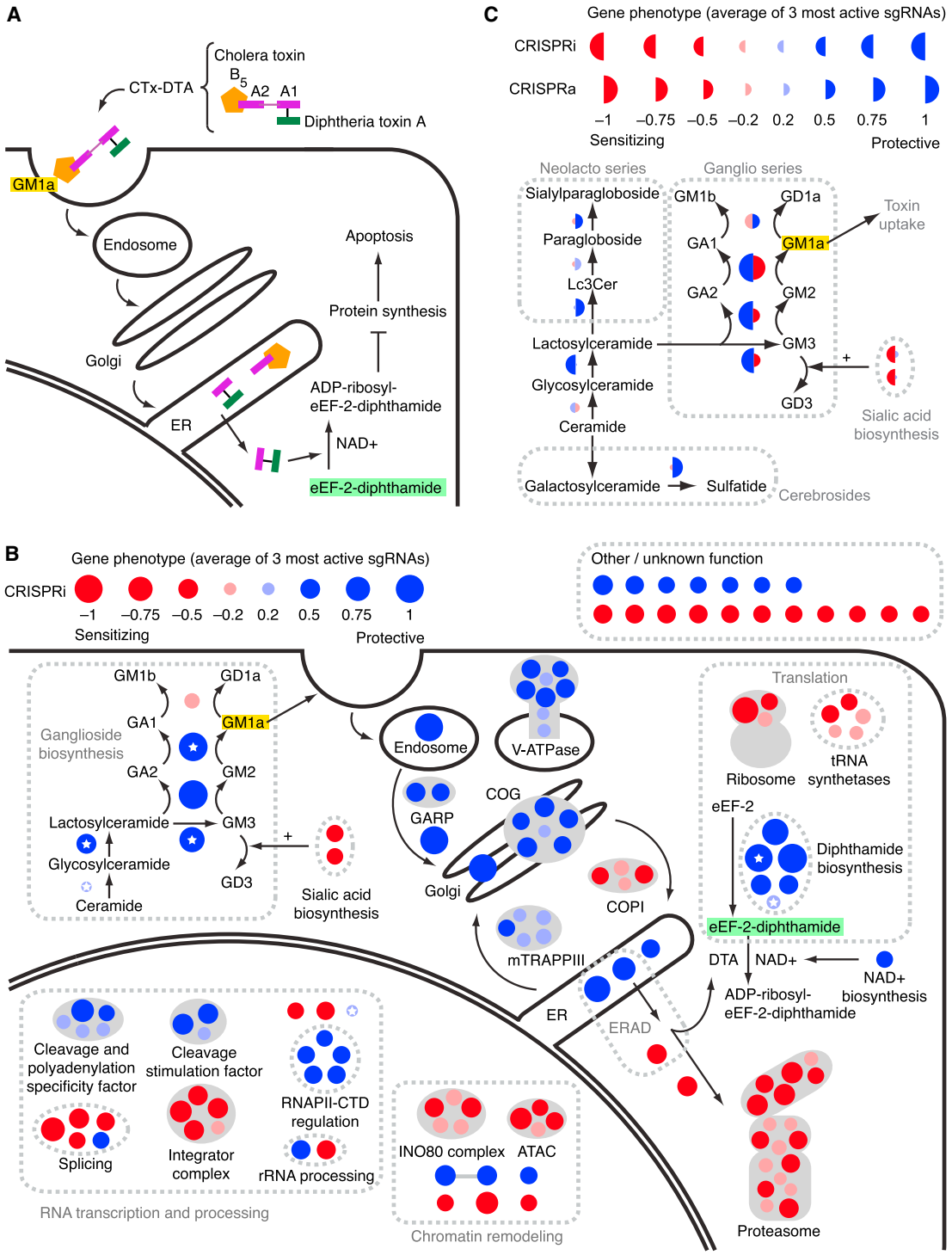

Figure 6. Genome-Scale CRISPRi and CRISPRa Screens Reveal Known and New Pathways and Complexes Governing the Response to a Cholera-Diphtheria Fusion Toxin

(A) Model for CTx-DTA binding, retrograde trafficking, retrotranslocation, and cellular toxicity.

(B) Overview of top hit genes detected by the CTx-DTA screen. Dark red and blue circles: Top 50 sensitizing and protective hits, respectively. Light red and blue circles: further hits that fall into the same protein complexes or pathways as top 50 hits. Circle area is proportional to phenotype strength. White stars denote genes identified in a previous haploid mutagenesis screen (Guimaraes et al., 2011). See also Figure S6 for hit gene names.

(C) CRISPRi and CRISPRa hits in sphingolipid metabolism. Display as in (B), except that the left and right sides of each circle represent the phenotypes in the CRISPRi and CRISPRa screens, respectively.

2011). Some aspects of both cholera and diphtheria toxin entry and toxicity are well characterized, but open questions remain. The cell surface receptor for cholera toxin is the GM1a ganglioside (Van Ness et al., 1980). After endocytosis, the toxin traffics via the Golgi to the endoplasmic reticulum (ER), from which it retrotranslocates into the cytosol, possibly through the ER-associated degradation (ERAD) machinery. Once in the cytosol, the DTA moiety ADP-ribosylates the diphthamide residue in Elongation Factor 2, halting translation and killing the cell (Figure 6A).

K562 cells expressing the CRISPRi sgRNA library and dCas9-KRAB were either grown under standard conditions or treated with several pulses of CTx-DTA over the course of 10 days. We observed highly correlated enrichment and depletion of many sgRNAs between replicates, indicating that CRISPRi can identify genes that modulate both resistance and sensitivity to a selective pressure (Table S2).

We ranked genes by the average phenotype of their three strongest sgRNAs (Table S3, and Figures 6B and S6). GSEA revealed that KEGG pathways enriched for top protective hit genes were "Infection with *Vibrio cholerae*" and "Glycosphingolipid biosynthesis, ganglio-series" (Figure S7B), while gene sets for top sensitizing genes included "ribosome" and "proteasome" (Figure S7B). Since the diphtheria toxin catalytic subunit inhibits translation, depletion of the ribosome can be expected to sensitize cells to the toxin. Disruption of the proteasome also sensitizes cells to CTx-DTA, suggesting that the cytosolic toxin is a substrate for proteasomal degradation. Taken together, the unbiased GSEA analysis provides support for the high specificity in hit gene identification by our CRISPRi approach.

We further defined the 50 hits with the strongest protective effect and the 50 hits with the strongest sensitizing effect as "top hits" (all of these phenotypes are far outside of the range seen with otherwise matched negative control sgRNAs). We characterized these genes by assigning them to cellular pathways and protein complexes according to their previously characterized roles (Figures 6B and S6). Our CRISPRi screen identified a protective effect of knockdown for all top hits recovered in the previously published haploid mutagenesis screen (white stars in Figure 6B). The two top pathways identified by haploid mutagenesis as modulating cellular sensitivity to CTx-DTA are the diphthamide biosynthetic pathway (required to generate eEF-2-diphthamide, the target of diphtheria toxin) and the ganglioside biosynthetic pathway (required to produce GM1a, the cell-surface receptor for cholera toxin). Our screen also identified many additional core components of each pathway. While knockdown of all hits in the diphthamide biosynthesis pathway had a protective effect, the results for ganglioside biosynthesis genes showed a more complex pattern: knockdown of enzymes involved in the production of GM1a were protective, whereas knockdown of enzymes that catalyze the production of other gangliosides (including GM1b) was sensitizing. These results provide genetic confirmation that GM1a is the relevant cell-surface receptor for CTx-DTA and more broadly illustrate the value of being able to reliably detect both sensitizing and protective genes to dissect biological pathways.

Many of the top hits are components of cellular pathways and protein complexes previously identified in experiments to be important for retrograde trafficking and retrotranslocation of other toxins such as ricin and Shiga toxin (Bassik et al., 2013; Smith et al., 2009). Retrotranslocation of the catalytic chain of CTx has been proposed to be mediated by the ER-associated degradation (ERAD) pathway, although this pathway was not identified in previous genetic screens. Consistent with this proposed role for the ERAD machinery, knockdown of members of the ERAD E3 ubiquitin ligase complex, *SYVN1* (encoding Hrd1) and *SEL1L* (the mammalian homolog of yeast Hrd3), rendered cells resistant to CTx-DTA. Factors that mediate cytosolic degradation of ERAD substrates (in particular *UBXN4*, also known as UBXD2 or erasin, and the proteasome) appeared as sensitizing hits, suggesting that they may reduce cytosolic levels of the toxin's catalytic subunit in WT cells.

To validate the suggested role of the identified ERAD factors in toxin retrotranslocation from the ER to the cytosol, we quantified the amount of CTx chains in the cytosol and membrane fractions. As expected, *SEL1L* knockdown resulted in a dramatic reduction of cytosolic CTx-A1, whereas levels in the membrane fraction were much less affected (Figures 7A–7C). By contrast, knockdown of *B4GALNT1*, an enzyme required for the synthesis of the CTx receptor GM1a, resulted in a nearly complete absence of CTx chains from both the cytosolic and the membrane fraction (Figures 7A–7C).

An open question in CTx biology is how the toxin traverses the Golgi network (Wernick et al., 2010). Our screen revealed that COG and GARP complexes, which tether late endosomes to the trans-Golgi network or modulate intra-Golgi retrograde transport (Bonifacino and Rojas, 2006) are critical host factors for CTx-DTA. These and other complexes and pathways we identify here (Figure 6B), including several involved in RNA processing, had not previously been linked to cholera toxin biology, highlighting the potential of CRISPRi as a discovery platform. Importantly, many top hits—even those not previously implicated in cholera or diphtheria pathogenesis—were tightly clustered in well-defined protein complexes and pathways. For several of these, the vast majority of components were hits, suggesting that CRISPRi screens can approach saturation.

Potent Phenotypes and Knockdown Levels Achieved by the Genome-Scale CRISPRi Library

To validate the results from this screen, we retested sgRNAs that putatively modulate cellular response to CTx-DTA in mechanistically diverse ways. For each sgRNA, we quantified both the ricin phenotypes as well as the change in abundance of the targeted transcript by qPCR. Our retest experiments were highly correlated with data from the primary screen (Figure 7D). In our validation experiments for the tiling ricin screen and the genome-scale CTx-DTA screen, the activities of 71 out of 72 sgRNAs were robustly confirmed and were highly correlated (R^2 = 0.879) with the results obtained in the primary screen. Finally, analysis of mRNA levels by qPCR data showed robust repression, with ~80%–99% knockdown for each sgRNA and at least 90% for every gene (Figure 7E).

A Genome-Scale CRISPRa Screen of Cholera-Diphtheria Toxin Complements and Extends CRISPRi Results

To further explore the biological insights gained from CRISPRa screening, we performed a genome-scale CRISPRa screen for

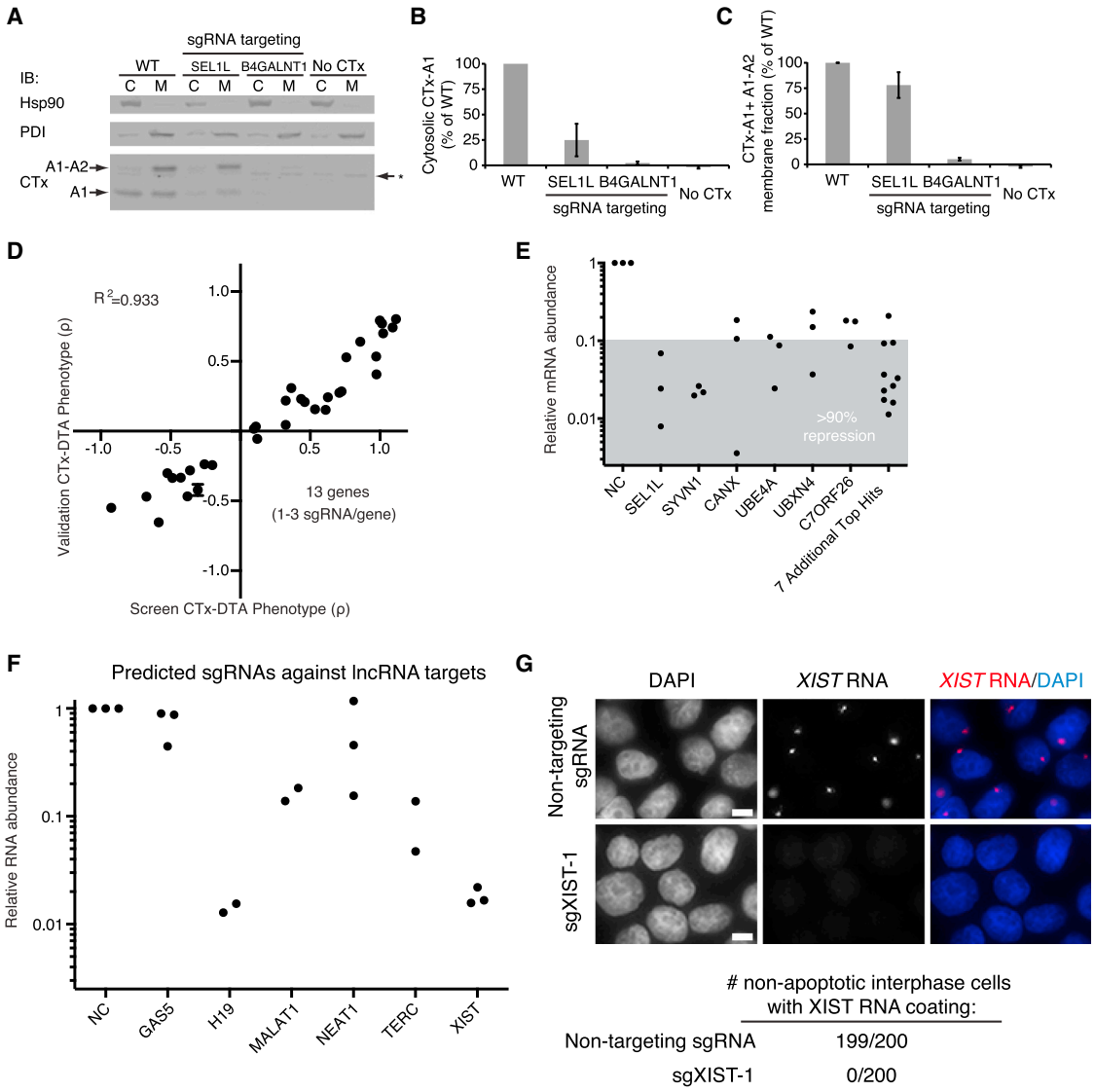

Figure 7. CRISPRi Strongly Represses Gene Expression of Both Protein-Coding and Noncoding Genes, Resulting in Reproducible Phenotypes

(A–C) Cells expressing a negative control sgRNA or an sgRNA targeting *SEL1L* or *B4GALNT1* were incubated with cholera toxin and fractionated to quantify cholera toxin present in the cytosolic and membrane fractions by western blot. *B4GALNT1* repression blocks toxin uptake, whereas *SEL1L* repression prevents toxin retrotranslocation from the membrane fraction to the cytosol.

(D) Validation of CTx-DTA screen phenotypes with single sgRNA retest experiments. Data are represented as the mean ± SD of replicates (n = 3).

(E) CRISPRi knockdown of 13 hit genes (28 sgRNAs; sgRNAs correspond to 7D) identified in the CTx-DTA screen was quantified by qPCR. The gray shaded region denotes sgRNAs showing at least 90% knockdown for each gene. Data are normalized to a negative control sgRNA (NC).

(F) CRISPRi knockdown of 6 lncRNA genes was quantified by qPCR. Two to three sgRNAs computationally predicted to target each gene were cloned and transduced into K562 cells expressing dCas9-KRAB. Data are normalized to a negative control sgRNA (NC).

(G) K562 cells expressing dCas9-KRAB were transduced with either a nontargeting sgRNA or an sgRNA targeting the *XIST* locus (sgXIST-1). The cells were then stained with DAPI and an RNA FISH probe for the *XIST* transcript. Two hundred nonapoptotic interphase cells in each condition were scored for *XIST* RNA coating. *XIST* is undetectable in cells transduced with sgXIST-1. Scale bar, 5 μm.

genes that modulate sensitivity to CTx-DTA (Tables S2 and S3). As with the CRISPRi screen, GSEA revealed the specificity of the detected hits (Figure S7B). For some of the top hits, CRISPR-mediated transcriptional activation and repression caused opposite phenotypes (e.g., enzymes in ganglioside biosynthesis, Figure 6C), similar to what we observed for genes controlling ricin sensitivity (Figure 3C).

CRISPRa also revealed additional and highly complementary information, as illustrated by analysis of glycosphingolipid biosynthesis pathways. Induction of enzymes in the neolacto branch of

sphingolipid biosynthesis protected cells from CTx-DTA (Figures 6C and S7A and S7C). This pathway is a parallel branch to the ganglioside branch, which produces the CTx-DTA receptor GM1a. Our findings suggest that upregulation of the neolacto branch diverts the common precursor lactosylceramide away from the ganglioside branch. Similarly, upregulation of the sulfatide-generating enzyme *GAL3ST1* has a protective effect, presumably by diverting ceramide from the sphingolipid to the cerebroside pathway (Figure 6C). These results highlight the capacity of CRISPRa to complement CRISPRi by querying the consequences of upregulating pathways that may otherwise be inactive.

Effective Knockdown of Noncoding RNAs

Finally, we investigated whether CRISPRi was able to repress the transcription of long noncoding RNAs (lncRNAs), a class of transcripts that have been difficult to systematically perturb by other methods (Bassett et al., 2014). Using our CRISPRi library design algorithm, we selected and cloned up to three sgRNAs each targeting six characterized lncRNAs (*GAS5*, *H19*, *MALAT1*, *NEAT1*, *TERC*, *XIST*) (Geisler and Coller, 2013) with good evidence of expression in K562 cells. We transduced the sgRNAs into cells expressing dCas9-KRAB and quantified the amount of transcript knockdown by qPCR. We achieved >80% knockdown for all but one of the lncRNA genes tested (Figure 7F). Overall, more than 50% of the sgRNAs yielded >85% knockdown. We confirmed the strong repression of *XIST* by RNA fluorescence in situ hybridization (FISH) and observed no residual expression along the X chromosome (Figure 7G). These results demonstrate that CRISPRi can effectively repress lncRNA expression, enabling future systematic studies of noncoding gene function.

DISCUSSION

Here, we establish CRISPRi and CRISPRa as robust tools for systematically manipulating transcription of endogenous genes in human cells. We demonstrate that CRISPRi/a can be used to rapidly screen for both loss-of-function and gain-of-function phenotypes in a pooled format. We identify both known and unexpected genes that control growth of K562 cells or that modulate sensitivity to a toxin (CTx-DTA). We also show that we can use CRISPRi/a to create allelic series of gene expression, spanning a broad range from ~100-fold repression to ~10-fold induction, allowing us to define how the abundance of a protein or transcript relates to its function.

A key feature of CRISPRi is the low incidence of off-target effects, as evidenced by the near-absence of activity for three large and distinct classes of negative control sgRNAs in our genome-scale CRISPRi library. This feature simplifies validation and interpretation of screening results. The observed specificity likely stems from two distinct properties of our system. First, CRISPRi/a complexes bound outside a narrow window around the TSS largely fail to modulate transcription; this dramatically shrinks the sequence space across the genome where off-target binding could produce significant off-target activity. Second, CRISPRi activity is highly sensitive to mismatches between the sgRNA and target DNA, suggesting that off-target binding of dCas9 observed in ChIP-seq experiments is too transient to impact transcription (Duan et al., 2014; Kuscu et al., 2014; Wu et al., 2014).

CRISPRa screening provides a new approach for exploring the diversity of transcripts across complex genomes. Gene activation has been used to dissect the limiting component of a biochemical process, identify the molecular target of a drug, or activate key rate-limiting steps in a pathway (Davis et al., 1987; Rine et al., 1983). Recently, a combinatorial cDNA overexpression screen identified genes that, when coexpressed, reprogram fibroblasts into pluripotent stem cells (Takahashi and Yamanaka, 2006). CRISPRa should greatly accelerate similar searches for combinations of factors with emergent properties. In addition, CRISPRa will likely provide insight into cellular pathways where redundancy hampers loss-of-function genetic approaches. CRISPRa will also enable the exploration of cellular states in which otherwise inactive pathways are induced, and thereby reveal functional coupling within complex cellular networks and suggest potential therapeutic strategies.

Our ability to control transcription with high specificity simplifies the analysis and validation of high-throughput screening data. The genome-scale CRISPRi and CRISPRa libraries described here contain 10 sgRNAs per TSS. The resulting library size allows each to be screened in a population of 200 million cells, which can be easily grown in a single spinner flask. Furthermore, the observed high specificity and an improved understanding of rules governing sgRNA activity should enable us to create even more compact sgRNA libraries. Additionally, an sgRNA library designed to activate or repress a broader range of transcripts in the human genome could reveal the function of many noncanonical RNAs encoded in the human genome. As most noncoding transcripts are nuclear and lack an open reading frame, methods that directly modulate transcription are optimally suited for interrogating the function of these RNAs (Derrien et al., 2012).

Systematic genetic interaction (GI) maps are powerful tools for revealing gene functions within pathways or complexes (Bassik et al., 2013; Boone et al., 2007; Costanzo et al., 2010). A CRISPRa GI map or a combined CRISPRi/a GI map could yield rich novel biology and help elucidate how networks of proteins dictate cellular function. More generally, quantitative methods of turning on and off one or multiple transcripts represent a critical tool for understanding how expression of the genes encoded in our genomes controls cell function and fate.

EXPERIMENTAL PROCEDURES

CRISPRi/a Libraries

Tiling Libraries

sgRNAs were designed targeting 49 genes (see Figure 1E) previously identified in shRNA screens as having ricin-resistance phenotype (Bassik et al., 2013). All possible sgRNAs within a 10 kb window around the gene TSS and meeting certain criteria were included (see Extended Experimental Procedures). Negative controls were designed based on scrambled sequences from these 10 kb windows and filtered by the same criteria as targeting sgRNAs.

Genome-Scale CRISPRi/a Libraries

Genes were selected from the entire set of protein-coding genes, although a subset of genes with a RPKM of 0 in a K562 cell RNA-seq expression data set were excluded. sgRNAs conforming to rules including low predicted off-targets and minimal length (see Figure S2 and Extended Experimental Procedures) were selected from a window of −50 to +300 bp (CRISPRi) or −400 to −50 bp (CRISPRa) with respect to the TSS. Negative controls we designed in the same way based on scrambled sequence derived from the same window of several hundred genes.

Library Cloning

Oligonucleotides encoding sgRNAs designed as described above were synthesized as pooled libraries. These were then cloned into lentiviral vectors for expression from a U6 promoter (see Extended Experimental Procedures).

Cell Line Construction

For constitutive and inducible CRISPRi screens, polyclonal cells expressing dCas9/KRAB fusion proteins driven from an SFFV or TRE3G promoter, respectively, were generated by viral transduction. For CRISPRa screens, a clonal cell line expressing dCas9-SunTag and a scFV-sfGFP-VP64 fusion was generated (See Extended Experimental Procedures).

Growth and Toxin Screens

Cells were grown at minimum library coverage of 1,000 for tiling screens and 3,750 for genome-scale screens. For growth screens, cells were grown in spinner flasks and harvested at 0 and 10 days after puromycin selection. For toxin screens, cells were treated with pulses of ricin or CTx-DTA (Bassik et al., 2013; Guimaraes et al., 2011) and harvested when sufficient selective pressure relative to untreated cells had been applied. Briefly, DNA was isolated, the cassette encoding the sgRNA was amplified by PCR, and relative sgRNA abundance was determined by next generation sequencing as previously described (Bassik et al., 2013; Kampmann et al., 2014).

SUPPLEMENTAL INFORMATION

Supplemental Information includes Extended Experimental Procedures, seven figures, and four tables and can be found with this article online at http://dx.doi.org/10.1016/j.cell.2014.09.029.

AUTHOR CONTRIBUTIONS

B.A., L.A.G., M.A.H., M.K., J.S.W. were primarily responsible for the conception, design, and interpretation of the experiments and wrote the manuscript. B.A., Y.C., L.A.G., M.A.H., M.K., J.E.V., and E.H.W. conducted experiments. L.A.G. cloned dCas9 chimeras and sgRNA expression constructs, constructed cell lines, carried out tiling screens, and conducted validation experiments. M.A.H. designed libraries, carried out tiling and genome-scale screens, and analyzed screen data. B.A. constructed the inducible cell line and conducted all inducible experiments. C.G. and H.L.P. contributed to CTx-DTA studies. B.P. contributed to *XIST* studies. M.C.B. and L.S.Q. contributed to the conception and interpretation of the experiments.

ACKNOWLEDGMENTS

The authors thank M. Tanenbaum, J. Tsai, K. Kostova, J. Zalatan, W. Lim, S. Weissman, J. Doudna, and R. Vale for unpublished reagents, technical advice and helpful discussion. L.S.Q. acknowledges support from the UCSF Center for Systems and Synthetic Biology. This work was supported by NIH P50 GM102706 (J.S.W.), NIH P50 GM081879 (L.S.Q., E.H.W.), NIH U01 CA168370 and NIH R01 DA036858 (J.S.W.), as well as the Howard Hughes Medical Institute (J.E.V., Y.C., M.K., M.A.H., J.S.W.). B.A. is an HHMI Fellow of the Damon Runyon Cancer Research Foundation (DRG-[2182-14]). L.A.G. is a Fellow of the Leukemia and Lymphoma Society. M.A.H. is supported by the UCSF Medical Scientist Training Program. M.K. is supported by NCI/NIH Pathway to Independence Award K99CA181494.

Received: July 15, 2014
Revised: September 3, 2014
Accepted: September 16, 2014
Published: October 9, 2014

REFERENCES

Adamson, B., Smogorzewska, A., Sigoillot, F.D., King, R.W., and Elledge, S.J. (2012). A genome-wide homologous recombination screen identifies the RNA-binding protein RBMX as a component of the DNA-damage response. Nat. Cell Biol. *14*, 318–328.

Alberich-Jordà, M., Wouters, B., Balastik, M., Shapiro-Koss, C., Zhang, H., Di Ruscio, A., Radomska, H.S., Ebralidze, A.K., Amabile, G., Ye, M., et al. (2012). C/EBPγ deregulation results in differentiation arrest in acute myeloid leukemia. J. Clin. Invest. *122*, 4490–4504.

Bassett, A.R., Akhtar, A., Barlow, D.P., Bird, A.P., Brockdorff, N., Duboule, D., Ephrussi, A., Ferguson-Smith, A.C., Gingeras, T.R., Haerty, W., et al. (2014). Considerations when investigating lncRNA function in vivo. eLife *3*, e03058.

Bassik, M.C., Lebbink, R.J., Churchman, L.S., Ingolia, N.T., Patena, W., LeProust, E.M., Schuldiner, M., Weissman, J.S., and McManus, M.T. (2009). Rapid creation and quantitative monitoring of high coverage shRNA libraries. Nat. Methods *6*, 443–445.

Bassik, M.C., Kampmann, M., Lebbink, R.J., Wang, S., Hein, M.Y., Poser, I., Weibezahn, J., Horlbeck, M.A., Chen, S., Mann, M., et al. (2013). A systematic mammalian genetic interaction map reveals pathways underlying ricin susceptibility. Cell *152*, 909–922.

Beerli, R.R., Segal, D.J., Dreier, B., and Barbas, C.F., 3rd. (1998). Toward controlling gene expression at will: specific regulation of the erbB-2/HER-2 promoter by using polydactyl zinc finger proteins constructed from modular building blocks. Proc. Natl. Acad. Sci. USA *95*, 14628–14633.

Beerli, R.R., Dreier, B., and Barbas, C.F., 3rd. (2000). Positive and negative regulation of endogenous genes by designed transcription factors. Proc. Natl. Acad. Sci. USA *97*, 1495–1500.

Bonifacino, J.S., and Rojas, R. (2006). Retrograde transport from endosomes to the trans-Golgi network. Nat. Rev. Mol. Cell Biol. *7*, 568–579.

Boone, C., Bussey, H., and Andrews, B.J. (2007). Exploring genetic interactions and networks with yeast. Nat. Rev. Genet. *8*, 437–449.

Carette, J.E., Guimaraes, C.P., Varadarajan, M., Park, A.S., Wuethrich, I., Godarova, A., Kotecki, M., Cochran, B.H., Spooner, E., Ploegh, H.L., and Brummelkamp, T.R. (2009). Haploid genetic screens in human cells identify host factors used by pathogens. Science *326*, 1231–1235.

Cech, T.R., and Steitz, J.A. (2014). The noncoding RNA revolution-trashing old rules to forge new ones. Cell *157*, 77–94.

Chang, K., Elledge, S.J., and Hannon, G.J. (2006). Lessons from Nature: microRNA-based shRNA libraries. Nat. Methods *3*, 707–714.

Costanzo, M., Baryshnikova, A., Bellay, J., Kim, Y., Spear, E.D., Sevier, C.S., Ding, H., Koh, J.L.Y., Toufighi, K., Mostafavi, S., et al. (2010). The genetic landscape of a cell. Science *327*, 425–431.

Davis, R.L., Weintraub, H., and Lassar, A.B. (1987). Expression of a single transfected cDNA converts fibroblasts to myoblasts. Cell *51*, 987–1000.

Derrien, T., Johnson, R., Bussotti, G., Tanzer, A., Djebali, S., Tilgner, H., Guernec, G., Martin, D., Merkel, A., Knowles, D.G., et al. (2012). The GENCODE v7 catalog of human long noncoding RNAs: analysis of their gene structure, evolution, and expression. Genome Res. *22*, 1775–1789.

Djebali, S., Davis, C.A., Merkel, A., Dobin, A., Lassmann, T., Mortazavi, A., Tanzer, A., Lagarde, J., Lin, W., Schlesinger, F., et al. (2012). Landscape of transcription in human cells. Nature *489*, 101–108.

Duan, J., Lu, G., Xie, Z., Lou, M., Luo, J., Guo, L., and Zhang, Y. (2014). Genome-wide identification of CRISPR/Cas9 off-targets in human genome. Cell Res. *24*, 1009–1012.

Gaj, T., Gersbach, C.A., and Barbas, C.F., 3rd. (2013). ZFN, TALEN, and CRISPR/Cas-based methods for genome engineering. Trends Biotechnol. *31*, 397–405.

Geisler, S., and Coller, J. (2013). RNA in unexpected places: long non-coding RNA functions in diverse cellular contexts. Nat. Rev. Mol. Cell Biol. *14*, 699–712.

Gilbert, L.A., Larson, M.H., Morsut, L., Liu, Z., Brar, G.A., Torres, S.E., Stern-Ginossar, N., Brandman, O., Whitehead, E.H., Doudna, J.A., et al. (2013). CRISPR-mediated modular RNA-guided regulation of transcription in eukaryotes. Cell *154*, 442–451.

Guimaraes, C.P., Carette, J.E., Varadarajan, M., Antos, J., Popp, M.W., Spooner, E., Brummelkamp, T.R., and Ploegh, H.L. (2011). Identification of host cell factors required for intoxication through use of modified cholera toxin. J. Cell Biol. *195*, 751–764.

Habedanck, R., Stierhof, Y.-D., Wilkinson, C.J., and Nigg, E.A. (2005). The Polo kinase Plk4 functions in centriole duplication. Nat. Cell Biol. *7*, 1140–1146.

Huang, L.C., Clarkin, K.C., and Wahl, G.M. (1996). Sensitivity and selectivity of the DNA damage sensor responsible for activating p53-dependent G1 arrest. Proc. Natl. Acad. Sci. USA *93*, 4827–4832.

Huang, W., Sherman, B.T., and Lempicki, R.A. (2009a). Systematic and integrative analysis of large gene lists using DAVID bioinformatics resources. Nat. Protoc. *4*, 44–57.

Huang, W., Sherman, B.T., and Lempicki, R.A. (2009b). Bioinformatics enrichment tools: paths toward the comprehensive functional analysis of large gene lists. Nucleic Acids Res. *37*, 1–13.

Jackson, S.P. (2002). Sensing and repairing DNA double-strand breaks. Carcinogenesis *23*, 687–696.

Jackson, A.L., Bartz, S.R., Schelter, J., Kobayashi, S.V., Burchard, J., Mao, M., Li, B., Cavet, G., and Linsley, P.S. (2003). Expression profiling reveals off-target gene regulation by RNAi. Nat. Biotechnol. *21*, 635–637.

Kampmann, M., Bassik, M.C., and Weissman, J.S. (2013). Integrated platform for genome-wide screening and construction of high-density genetic interaction maps in mammalian cells. Proc. Natl. Acad. Sci. USA *110*, E2317–E2326.

Kampmann, M., Bassik, M.C., and Weissman, J.S. (2014). Functional genomics platform for pooled screening and generation of mammalian genetic interaction maps. Nat. Protoc. *9*, 1825–1847.

Koike-Yusa, H., Li, Y., Tan, E.-P., Velasco-Herrera, Mdel.C., and Yusa, K. (2014). Genome-wide recessive genetic screening in mammalian cells with a lentiviral CRISPR-guide RNA library. Nat. Biotechnol. *32*, 267–273.

Kuscu, C., Arslan, S., Singh, R., Thorpe, J., and Adli, M. (2014). Genome-wide analysis reveals characteristics of off-target sites bound by the Cas9 endonuclease. Nat. Biotechnol. *32*, 677–683.

Mittler, G., Stühler, T., Santolin, L., Uhlmann, T., Kremmer, E., Lottspeich, F., Berti, L., and Meisterernst, M. (2003). A novel docking site on Mediator is critical for activation by VP16 in mammalian cells. EMBO J. *22*, 6494–6504.

Qi, L.S., Larson, M.H., Gilbert, L.A., Doudna, J.A., Weissman, J.S., Arkin, A.P., and Lim, W.A. (2013). Repurposing CRISPR as an RNA-guided platform for sequence-specific control of gene expression. Cell *152*, 1173–1183.

Rine, J., Hansen, W., Hardeman, E., and Davis, R.W. (1983). Targeted selection of recombinant clones through gene dosage effects. Proc. Natl. Acad. Sci. USA *80*, 6750–6754.

Sander, J.D., and Joung, J.K. (2014). CRISPR-Cas systems for editing, regulating and targeting genomes. Nat. Biotechnol. *32*, 347–355.

Shalem, O., Sanjana, N.E., Hartenian, E., Shi, X., Scott, D.A., Mikkelsen, T.S., Heckl, D., Ebert, B.L., Root, D.E., Doench, J.G., and Zhang, F. (2014). Genome-scale CRISPR-Cas9 knockout screening in human cells. Science *343*, 84–87.

Sigoillot, F.D., Lyman, S., Huckins, J.F., Adamson, B., Chung, E., Quattrochi, B., and King, R.W. (2012). A bioinformatics method identifies prominent off-targeted transcripts in RNAi screens. Nat. Methods *9*, 363–366.

Smith, R.D., Willett, R., Kudlyk, T., Pokrovskaya, I., Paton, A.W., Paton, J.C., and Lupashin, V.V. (2009). The COG complex, Rab6 and COPI define a novel Golgi retrograde trafficking pathway that is exploited by SubAB toxin. Traffic *10*, 1502–1517.

Spitz, F., and Furlong, E.E.M. (2012). Transcription factors: from enhancer binding to developmental control. Nat. Rev. Genet. *13*, 613–626.

Takahashi, K., and Yamanaka, S. (2006). Induction of pluripotent stem cells from mouse embryonic and adult fibroblast cultures by defined factors. Cell *126*, 663–676.

Tanenbaum, M.E., Macurek, L., van der Vaart, B., Galli, M., Akhmanova, A., and Medema, R.H. (2011). A complex of Kif18b and MCAK promotes microtubule depolymerization and is negatively regulated by Aurora kinases. Curr. Biol. *21*, 1356–1365.

Tanenbaum, M.E., Gilbert, L.A., Qi, L.S., Weissman, J.S., and Vale, R.D. (2014). A versatile protein tagging system for signal amplification in single molecule imaging and gene regulation. Cell *159*, this issue, 635–646.

Van Ness, B.G., Howard, J.B., and Bodley, J.W. (1980). ADP-ribosylation of elongation factor 2 by diphtheria toxin. Isolation and properties of the novel ribosyl-amino acid and its hydrolysis products. J. Biol. Chem. *255*, 10717–10720.

Vogelstein, B., Papadopoulos, N., Velculescu, V.E., Zhou, S., Diaz, L.A., Jr., and Kinzler, K.W. (2013). Cancer genome landscapes. Science *339*, 1546–1558.

Wang, T., Wei, J.J., Sabatini, D.M., and Lander, E.S. (2014). Genetic screens in human cells using the CRISPR-Cas9 system. Science *343*, 80–84.

Wernick, N.L.B., Chinnapen, D.J.-F., Cho, J.A., and Lencer, W.I. (2010). Cholera toxin: an intracellular journey into the cytosol by way of the endoplasmic reticulum. Toxins (Basel) *2*, 310–325.

Wu, X., Scott, D.A., Kriz, A.J., Chiu, A.C., Hsu, P.D., Dadon, D.B., Cheng, A.W., Trevino, A.E., Konermann, S., Chen, S., et al. (2014). Genome-wide binding of the CRISPR endonuclease Cas9 in mammalian cells. Nat. Biotechnol. *32*, 670–676.

Zhang, P., Zhang, X., Iwama, A., Yu, C., Smith, K.A., Mueller, B.U., Narravula, S., Torbett, B.E., Orkin, S.H., and Tenen, D.G. (2000). PU.1 inhibits GATA-1 function and erythroid differentiation by blocking GATA-1 DNA binding. Blood *96*, 2641–2648.

Zhang, F., Cong, L., Lodato, S., Kosuri, S., Church, G.M., and Arlotta, P. (2011). Efficient construction of sequence-specific TAL effectors for modulating mammalian transcription. Nat. Biotechnol. *29*, 149–153.

Zhao, M., Sun, J., and Zhao, Z. (2013). TSGene: a web resource for tumor suppressor genes. Nucleic Acids Res. *41* (Database issue), D970–D976.